

A Study on the Removal of Zinc from Aqueous Solution using Chemically Activated Agave Sisalana Fibre

Helen Kalavathy.M^{1*} and Lima Rose Miranda²

¹Department of Chemical Engineering, Sriram Engineering College, Perumalpattu

²Department of Chemical Engineering, A.C.College of Technology,
Anna University, India

*Corres.author : helenkalavathy@gmail.com

Abstract: Agave sisalana fibre (ASF), a bio-waste has been demonstrated to be an effective material for the preparation of activated carbon (AC) for the removal of an inorganic pollutant such as zinc from wastewaters by adsorption. Fourier Transform Infrared Spectroscopy (FTIR) and scanning electron microscopy (SEM) were used to characterize the ASF. The various operating parameters such as contact time, pH, initial Zn ion concentration, carbon loading and temperature were studied. The optimum pH value for maximum adsorption was found to be 6. Thermodynamic parameters such as Gibbs free energy, enthalpy and entropy were calculated to understand the nature of adsorption. The equilibrium data were satisfactorily fitted to Langmuir, Freundlich and Temkin isotherms. The kinetic data fits to pseudo second order model with correlation coefficients greater than 0.999. The intra-particle diffusion rate constants and diffusion coefficient for different temperatures were evaluated and discussed. The studies showed that the Agave sisalana fibre can be used as an efficient adsorbent material for the removal of zinc from industrial effluents.

Introduction

Increasing application of heavy metals in industrial process has been resulted in production of massive effluents with huge amounts of toxic heavy metals. Due to increasing amounts of discharge and presence of these pollutants (heavy metals) which are toxic and have other negative effects on receptive waters in environment, has created great concerns. Unlike the organic compounds, these pollutants are non-degradable and tend to bio-accumulation in living organisms. Some of the heavy metals which have adverse effects are lead, arsenic, mercury, cadmium, copper, nickel, zinc. Among these metals Zinc is used most often in industries to produce stainless steel, metallic alloys, chargeable batteries, catalysers, coins, casting and metallurgy, electro-plating, metal-accumulator manufacturing¹. They enter into environment through natural ways and by human activities and cause pollution in environment. Zn in trace concentrations are among necessary elements and function as micronutrients in human body. However, in high concentration they cause problems for human such as stomach pain, skin burn, vomiting and nausea, anemia, cancer, cardiopulmonary disorders, asthma, chronic bronchitis, brain damage etc². Due to health concerns, potential toxicity and also increasing exposure of humans by Zn, several organizations have recommended guidelines. According to World Health Organization (WHO) maximum concentration limit for Zn in drinking water is 3 mg L⁻¹³.

Conventional methods such as precipitation, coagulation, electro dialysis, reverse osmosis (RO), ultra filtration, solvent extraction, ion-exchange, adsorption and bio-sorption, etc. have been developed for the removal of the heavy metals from wastewater. The disadvantage with precipitation is sludge production⁴. Ion-

exchange is not economical because of high operational costs. The disadvantage in RO is the amount of water wasted by the process and also high costs. The disadvantage in electro-dialysis is the formation of metal hydroxides, which clog the membrane. The disadvantage in bio-sorption is that it takes a long time for removal of metals. The disadvantage in ultra filtration is its poor efficiency and it needs a large pressure difference⁵. Adsorption methods do offer the most direct and economical method of treating water. Adsorption onto activated carbon has been applied successfully for the treatment of municipal and industrial wastewater and drinking water⁶. Successful removal of heavy metals from aqueous solutions using activated carbon is very economical. AC surfaces have a pore size that determine its adsorption capacity, a chemical structure that influences its interaction with polar and non-polar adsorbates, and active sites which determine the type of chemical reactions with other molecules.

There are many adsorbents used in the removal of heavy metal from industrial effluents. Agave sisalana is one of the cheap and effective adsorbent. This agave sisalana plant is readily available at Chhattisgarh, Madhya Pradesh, Karnataka and other states in India.

Activated carbon can be prepared by two methods, physical activation and chemical activation. The chemical activation can be performed in a single step and at relatively at low temperature, hence it is advantageous when compared to physical activation. The chemical agent promotes the formation of cross-links, leading to the formation of a rigid matrix that is further less prone to volatile loss and volume contraction upon heating to high temperatures⁷. Compared to zinc chloride, phosphoric acid is preferred because of the problems of corrosion, inefficient chemical recovery, and environmental disadvantages. It is well known that activation with phosphoric acid develops micro porosity when using cellulosic and lingo-cellulosic precursors in the manufacture of activated carbon. Chemical activation is carried out in two steps, in the first one the precursor is impregnated with phosphoric acid and in the second the heat treatment influences the carbonization process, generating the porosity, which becomes accessible when phosphoric acid is removed by washing. Consequently, the modification of chemical-precursor ratio permits the adjustment of porosity in the activated carbon.

In the present work, an attempt has been made to develop an inexpensive adsorbent system for the removal of zinc from aqueous solution using Agave sisalana fibre (sisal). This work investigates the potential of Activated carbon prepared from Agave sisalana in the removal of zinc ions from aqueous solutions.

Materials and methods

Preparation of adsorbent

ASF were collected and cut into small pieces. By washing with boiling water, water soluble and coloured components were removed from the samples and this was repeated till the water was virtually colourless. It was then washed with distilled water and dried in a hot air oven at 383K till it reaches constant weight. Then at an impregnation ratio of 1:2 (weight of sisal fiber : weight of phosphoric acid) sample was mixed with the phosphoric acid and after that it was soaked for 24 h so that the reagents were fully adsorbed onto the raw material. The mixture was dried at 383K for 1.5 h and then transferred to a sealed ceramic container. In a muffle furnace at 673K for a period of 1 h the dried mixture was activated. The activated carbon thus produced from ASF was then repetitively washed with distilled water to recover all the acid and then with 1% NaHCO₃ solution to remove the residual acid⁸. Then the activated carbon was powdered, sieved and the fraction which passed through 200 mesh screen were collected and stored in sealed containers.

Characterization of Activated Carbon

Activated carbons prepared from ASF are characterized by finding out its yield, bulk density, pH_{PZC}⁹, iodine number¹⁰, methylene blue number¹¹, methyl violet number, specific surface area, total pore volume and cation exchange capacity¹². To determine the amount of moisture, volatile matter, fixed carbon and ash content, proximate analysis of the raw materials and activated carbons were carried out. The proximate analysis of raw materials and AC were determined from thermo gravimetric analysis.

The surface morphology was studied to observe the pore development. In order to observe the surface morphology of the adsorbent, a scanning electron microscopic analysis was employed in this study. SEM images were recorded using JEOL JSM-6360, Japan, field emission SEM.

The surface functional groups of both the raw materials and the activated carbons produced were identified using Fourier transform infrared spectrophotometer. Fourier transform infrared spectra were obtained using a spectroscope (Tensor 29, Bruker) at a resolution of 1 cm^{-1} . Pressed potassium bromide (KBr) pellets at a sample/KBr weight ratio of 1:100 were scanned and recorded between 4000 and 400 cm^{-1} .

Synthetic Wastewater Preparation

Synthetic waste water solution was prepared by dissolving analytical grade $\text{ZnSO}_4 \cdot 7\text{H}_2\text{O}$ in distilled water to obtain a stock solution of 1000 mg L^{-1} metal solution. The working solution was diluted to the required concentration for experiments. By using sulphuric acid and sodium hydroxide the pH of the solutions was adjusted. All chemicals used were of analytical grade, which were used for the analysis of metal ions.

Batch Adsorption Studies

A series of 250 mL capacity Erlenmeyer flasks containing desired amount of zinc ion solutions of known concentrations and activated carbon produced from ASF (ACAS) were agitated in a temperature controlled shaker (Orbital Scigenics) at 180 rpm. The effect of contact time (0–240 min), initial zinc ion concentration ($10 - 50\text{ mg L}^{-1}$), solution pH (2.0–10), carbon dose ($0.05 - 0.7\text{ g (100 mL)}^{-1}$), and temperature ($293 - 323\text{ K}$) were studied. The pH of the solutions was adjusted using H_2SO_4 or NaOH . Samples were taken at prescribed time intervals; the solutions were centrifuged and the supernatant was analyzed for zinc ion concentration using UV spectrophotometer (Shimadzu Model UV-2100S) at 535 nm . The amount of metal ion adsorbed at any time t , was calculated using the equation.

$$q_t = \frac{(C_0 - C_t)V}{M} \quad (1)$$

where V is the adsorbate volume (L), M the amount of ACAS (g) and C_0 and C_t (mg L^{-1}) are the initial concentration of zinc ion and concentration of zinc ion at any time t , respectively.

Results and discussion

Characterization of the adsorbents

Proximate analysis

Table 1: Proximate analysis of RAS and ACAS

Characteristics	RAS	ACAS
Moisture (%)	12.41	4.22
Volatile matter (%)	5.84	7.37
Carbon (%)	75.91	78.59
Ash (%)	10.84	9.82

Table 2: Bulk density of Raw materials and AC samples

Samples	Bulk density (g mL^{-1})
RAS	0.3154
ACAS	0.4129

The proximate analysis of the raw materials and ACAS are given in (Table- 1). The bulk density of the raw materials and ACAS are shown in (Table- 2). Bulk density is defined as the mass of a unit volume of the sample in air, including both the pore system and the voids among the particles. It is very useful for the estimation of the packing volume or to determine the grade of carbon needed for an existing system.

Properties of Activated Carbon

The values of yield, pH_{PZC} , iodine number, methylene blue number, methyl violet number, specific surface area, total pore volume and cation exchange capacity(CEC) obtained for ACAS was compared with commercial activated carbon (CAC) and are summarized in (Table- 3).

Table 3: Characteristics of activated carbon samples

AC	Yield (%)	pH _{PZC}	Iodine number (mg g ⁻¹)	Methy-lene Blue number (mg g ⁻¹)	Methyl violet number (mg g ⁻¹)	Surface Area (m ² g ⁻¹)	Pore volume (cm ³ g ⁻¹)	CEC m eq (100 g) ⁻¹
CAC	-	6.67	834.02	210	125	482.21	0.3187	19.27
ACAS	49.34	6.65	1110.89	180	160	775.66	0.5387	23.19

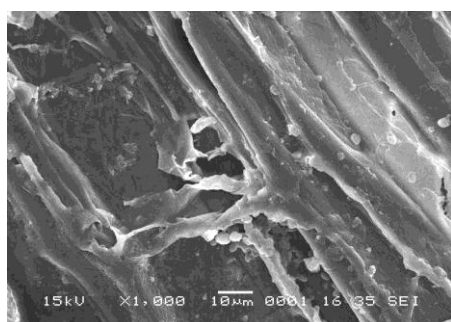
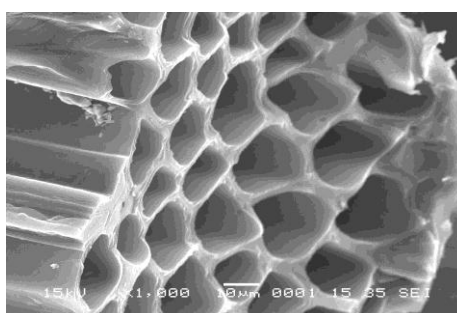
The surface charge is a function of pH. The pH at which the charge of the solid surface is zero has been referred to as the point of zero charge (pH_{pzc}). Above pH_{pzc} the surface charge of the carbon samples were negative and those below pH_{pzc} surface charge of the carbon samples were positive.

The iodine number is a measure of the porosity of activated carbon and it has been defined as the milligrams of iodine adsorbed per gram of carbon. The iodine number represents the surface area contributed by the pores larger than 10 Å^{13,14}. The iodine number has been commonly used in industry as a rough estimate of the surface area of the activated carbon. It is an indication of the internal surface area of the carbon.

Methylene blue and methyl violet numbers indicate the development of mesopores in the activated carbon and have been defined as the milligrams of methylene blue and methyl violet adsorbed per gram of carbon. Larger these numbers better was the availability of the AC to adsorb large molecules having similar dimensions to those methylene blue and methyl violet. The iodine number and methyl violet number values are higher for ACAS indicating the presence of more micro pores and macro pores when compared to CAC. The higher iodine number of ACAS, an indication of better micropore development thereby leading to large surface area and pore volume has been reflected in the values obtained.

Cation is an ion with a positive electrical charge. The CEC is the number of equivalents of exchangeable charge per mass of adsorbent. It is a measure of the adsorbent's capacity to exchange ions and has been expressed as milligram equivalents per 100 grams of adsorbent. Cations have the ability to be exchanged for another positively charged ion from the surfaces of the adsorbents.

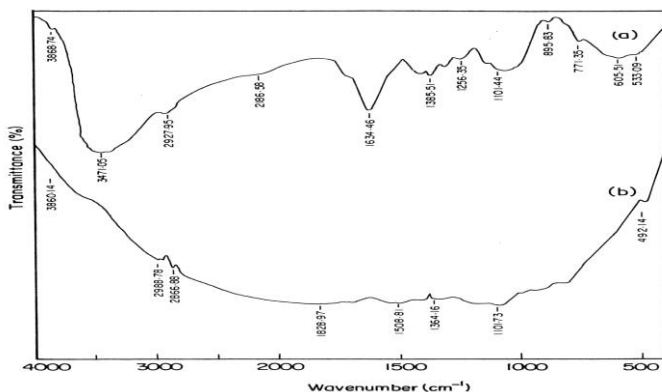
Scanning Electron Micrographs of Agave Sisalana

Figure 1: SEM of RAS**Figure 2: SEM of ACAS**

The microstructures of the RAS and ACAS are shown in (Figures- 1 & 2). As can be observed from (Figure- 1), the RAS surface exhibits many thin sheets or layers within the structure. The surface of the RAS presents large amounts of white agglomerates, probably inorganic matter. After impregnation, the amount of this white colour material decreased, giving rise to more fragmentary structures. The scanning electron micrographs obtained after activation (Figure- 2) showed a well developed porous structure. The activation process resulted in the creation of pores and a substantial removal of inorganic material. The cylindrical pores (with large openings) with more or less uniform pore size can be seen in the micrographs.

FTIR Of Agave Sisalana Fiber

Fourier Transform Infrared spectroscopy provides information on the surface chemistry of the adsorbent material. The surface functional groups of both the raw materials and the activated carbons prepared were analysed using FTIR. The FTIR of RAS (Figure- 3a) showed the presence of the following functional group.

Figure 3: FTIR spectra of (a) RAS and (b) ACAS

A broad band located around 3471.05 cm^{-1} is typically attributed to the hydroxyl groups or adsorbed water. A weak band at 2927.25 cm^{-1} is usually caused by the stretching vibration of the C-H alkane group. A band at a wave number of 2186.58 cm^{-1} indicated stretching vibration of $\text{-C}\equiv\text{N}$ and $\text{C}\equiv\text{C}$ group. A strong peak located at 1634.46 cm^{-1} can be assigned to the aromatic ring or the $\text{C}=\text{C}$ stretching vibration. A relatively low intensity peak at 1385.51 cm^{-1} can be attributed to the COO^- carboxylate group. A relatively weak band around 1258.35 cm^{-1} indicates the presence of COOH . A broad band at 1101.44 cm^{-1} can be ascribed to the asymmetric stretching of Si-O bond. A very small peak at 771.35 indicates aromatic hydrocarbons of disubstituted 1, 2 benzenes.

No peaks were observed corresponding to any functional group for ACAS (Figure 3b). The disappearance of the above mentioned groups may be due to hydrolysis effect of H_3PO_4 , resulting in the decomposition of these groups and subsequent release of their by-products as volatile matter. This proves that there were no functional groups on the surface of all the AC prepared and that they are only elemental carbons. Therefore, the removal of zinc from aqueous solutions using the AC is not due to the complex formation with surface functional groups but purely by adsorption, a surface phenomenon.

Batch Adsorption Studies for Zinc

The extent of adsorption of zinc ions onto ACAS was studied taking into consideration the following effects. As the adsorption process proceeds, the adsorbed metal ions tend to desorb back into the solution. Eventually the rate of adsorption and desorption would attain an equilibrium state. The time at which this adsorption equilibrium occurs was determined by studying the effect of contact time on the adsorption capacity. pH is one of the main variables which affected the adsorption process. The optimum pH value for the zinc removal has to be determined. Therefore, the effect of pH on the adsorption capacity was studied. Similarly, the effect of various other parameters such as initial zinc ion concentration, carbon loading and temperature were studied in order to optimize the operating variables.

Effect of Contact Time

The effect of contact time on adsorption capacity of ACAS for Zn adsorption is shown in (Figure- 4). The time for attaining equilibrium was found to be 3h. Further, an increase in the contact time did not show any significant change in the adsorption capacity.

Figure 4: The effect of contact time on adsorption capacity of ACAS for Z adsorption, ACAS loading $0.2\text{ g (100 mL)}^{-1}$, temperature 303 K , pH $5.62 - 5.81$

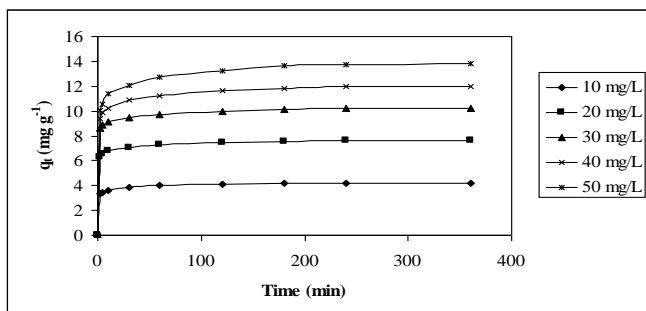
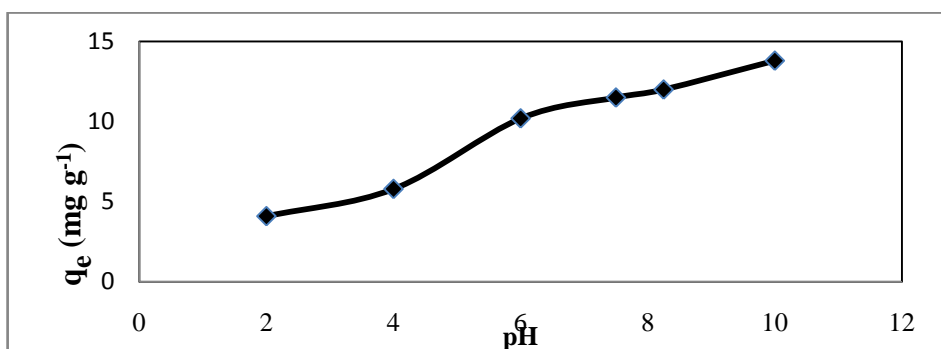


(Figure- 4) indicate that the rate of Zn removal by ACAS from the aqueous solutions of different concentration follow nearly similar trends. The initial rate of adsorption being very high during the first few minutes and then gradually dropping to zero as the equilibrium time was reached. As an approximation, the removal of zinc ions could be said to take place in two distinct steps: a relatively fast one followed by a slower one. This behaviour is due to the larger surface area of the activated carbon samples being available for the adsorption of zinc ions. Once the external surface area of the activated carbon is occupied by the zinc ions, then with time, the metal uptake rate is controlled by the rate at which the adsorbate is transported from the exterior to the interior sites of the adsorbent¹⁵. The necessary time to reach this equilibrium is about 3 h. Increasing the removal time to 6 h did not show notable increase in the adsorption. It can also be observed from the figure that the change in the initial concentration of the metal ions did not affect the time at which the equilibrium was attained. Therefore, to carry out all the experiments at a uniform time period, the equilibrium time was taken as 4 h. For further studies, the time for attaining equilibrium was set at 4 h.

Effect of pH

Figure 5: The effect of pH on adsorption capacity of ACAS for Zn adsorption, Initial Zn ion Concentration 30 mg L⁻¹, AC loading 0.2 g (100 mL)⁻¹, temperature 303 K, contact time 4h



The effect of pH on adsorption capacity of ACAS was studied at 303 K by varying the initial pH of metal ion solution from 2 to 12 for a constant carbon loading of 0.2 g / 100 ml of solution containing 30 mg of metal ions per litre of solution. The effect of pH on the adsorption capacity is shown in Figure 5. The adsorption experiments were conducted for the equilibration time of 4 h. The pH of the aqueous solution is an important controlling parameter in the adsorption process¹⁶. The percentage removal of metal ions was found to increase with increasing pH, showing maximum adsorption capacity at pH 10. The optimum initial pH was chosen as 6 because precipitation of the metal hydroxide was observed at pH greater than 6. It was observed that the adsorption was very low in the pH range of 2-4. On increasing the pH above 6, the adsorption capacity rapidly increased. This phenomenon can be explained by the increased surface charge of the ACAS together with the precipitation of the metal ions thereby decreasing the metal ion content in the supernatant solution.

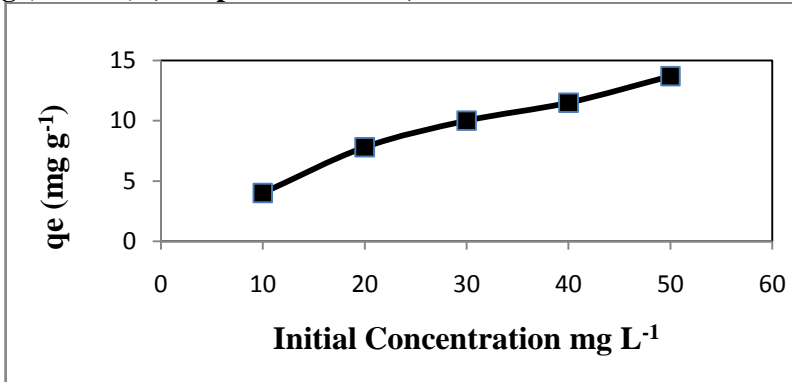
The surface charge of AC was found to be a strong function of pH. The pH_{PZC} of ACAS was found to be 6.65. At pH value below pH_{PZC} , the surface charge of the carbon samples was positive and hence the adsorption capacity decreased. The decrease in the metal uptake at low pH was due to the fact that the H^+ ions competed with the metal ions for the active sites on the adsorbent and thereby lowered the adsorption capacity for metal adsorption¹⁷. At pH value above pH_{PZC} , surface of the carbon samples have a higher negative charge which results in higher attraction of metal ions (cations). Therefore, an increase in pH showed increased metal adsorption, in which the surface of the activated carbon finds less H^+ ions competing for the adsorption sites. In this case adsorption occurred by electrostatic force of attraction between the metal ions and the surface of the adsorbent¹⁸. A pH of 6 was chosen as the optimum pH and all the experiments were therefore carried out at pH 6.

Effect of Initial Concentration

The performance of the AC sample based on their adsorption capacities gives a much clearer picture as the adsorption capacity represents the mg of adsorbate adsorbed per g of the adsorbent. The effect of the initial metal ion concentration on the adsorption capacity of ACAS for the adsorption of Zn is presented in Figure 6. The experiments were carried out at pH 6, at the temperature of 303 K for a period of 4h, with a constant carbon loading of 0.2 g / 100mL of solution containing different concentration of the metal ions. As can be seen the adsorption capacity of all the carbon samples increased with an increase in the initial concentration of metal

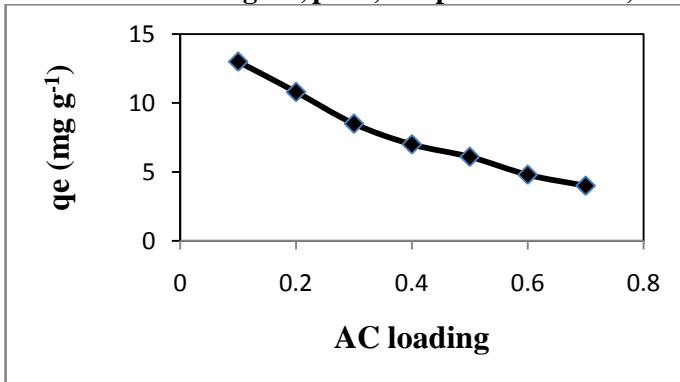
ions. As the concentration of the adsorbate increased, the numbers of sites for adsorption remaining the same, the availability of free sites for adsorption decreased. The amount of zinc uptake per unit weight of the adsorbent increased with an increase in the initial zinc ion concentration and showed a maximum adsorption capacity of 13.78 mg g^{-1} . The increase in the adsorption capacity with an increase in the initial metal ion concentration is due to the fact that, at higher initial concentrations, the ratio of the initial number of moles of metal ions to the available adsorption surface area was high. This may be attributed to an increase in the driving force of the concentration gradient with an increase in the initial metal concentration¹⁹.

Figure 6: The effect of initial Zn concentration on adsorption capacity of ACAS, pH 6, AC loading $0.2 \text{ g (100 mL)}^{-1}$, temperature 303 K, contact time 4h



Effect of Activated Carbon Loading

Figure 7: The effect of AC loading on adsorption capacity of ACAS for Zn adsorption, Initial Zn ion concentration 30 mg L^{-1} , pH 6, temperature 303 K, contact time 4h

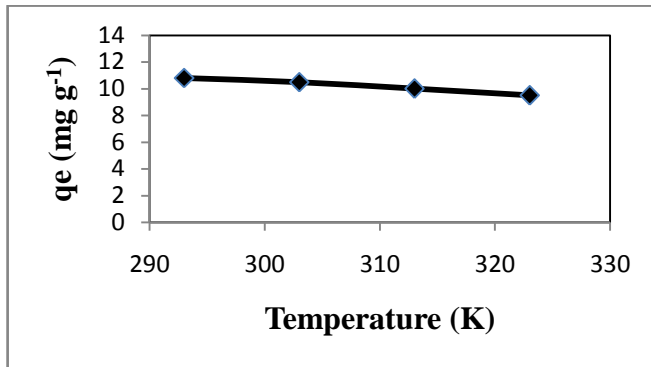


To determine the necessary activated carbon quantity required for the maximum removal of metal ions, the effect of activated carbon loading on the percentage removal was studied. The adsorption studies were carried out at pH 6, temperature 303 K for a retention period of 4 h, taking 100 mL of 30 mg L^{-1} of metal ion solution for various activated carbon loading. The effect of carbon loading on the adsorption capacity of ACAS is presented in Figure 7. The adsorption capacity decreased from 12.97 to 4.11 mg g^{-1} when carbon loading was increased from 0.1 to $0.7 \text{ g (100 mL)}^{-1}$. This is due to the fact that at higher carbon loading, the metal ion concentration in the solution dropped to a lower value and the system reached equilibrium at lower values of ' q_e ' indicating that the adsorption sites remain unsaturated²⁰.

Effect of Temperature

(Figure- 8) shows the relationship between temperature and adsorption capacity of ACAS. The experiments were carried out for a known concentration (30 mg L^{-1}) of metal ion solution, for a contact time of 4 h at pH 6 with constant carbon loading of $0.2 \text{ g (100 mL)}^{-1}$ of solution containing metal ions at different temperatures. The reduction in the adsorption capacity of ACAS with temperature for Zn adsorption from 10.58 to 9.24 mg g^{-1} show that the adsorption is an exothermic process.

Figure 8. The effect of temperature on adsorption capacity of ACAS for Zn adsorption, Initial Zn ion concentration 30 mg L⁻¹, AC loading 0.2 g (100 mL)⁻¹, pH 6, contact time 4h



The reduction in the adsorption capacity was due to the fact that the adsorbed molecules have greater vibrational energies and was therefore more likely to desorb from the surface.

The adsorption equilibrium data obtained for different temperatures were used to calculate the important thermodynamic properties such as standard Gibbs free energy (ΔG°), standard enthalpy change (ΔH°) and standard entropy change (ΔS°)²¹. The standard Gibbs free energy was evaluated by

$$\Delta G^\circ = -RT \ln K_c \quad (2)$$

The equilibrium constant K_c was calculated using the relationship

$$K_c = \left[\frac{C_{Be}}{C_{Ae}} \right] \quad (3)$$

where, C_{Be} and C_{Ae} are the equilibrium concentration of metal ions on the adsorbent and solution (mg L⁻¹), respectively.

The standard enthalpy (ΔH°) and entropy (ΔS°) of adsorption were determined from the Van't Hoff equation,

$$\ln K_c = \left[\frac{\Delta S^\circ}{R} - \frac{\Delta H^\circ}{RT} \right] \quad (4)$$

where, ΔH° and ΔS° were obtained from the slope and intercept of the Van't Hoff's plot of $\ln K_c$ versus $1/T$.

The thermodynamic parameters at different temperatures are listed in (Table- 4).

Table 4: Thermodynamic parameters for the adsorption of Zn on ACAS

T (K)	ΔG° (kJ mol ⁻¹)	ΔH° (kJ mol ⁻¹)	ΔS° (kJ mol ⁻¹ K ⁻¹)
293	-2.1269	-10.168	-0.02732
303	-1.9027		
313	-1.7221		
323	-1.2668		

The negative values of ΔG° had shown that the adsorption of Zn on ACAS are feasible and spontaneous. Moreover the free energy change becomes less negative indicating an exothermic process.

The values of ΔG° obtained in this work, indicates that electrostatic attraction is the major mechanism responsible for the zinc ion adsorption on ACAS. The values of ΔH° are negative, indicating that the adsorption process is exothermic in nature. The negative values of ΔS° indicate greater order of reaction during the adsorption of Zn on ACAS.

Adsorption Isotherms

The most widely used isotherm models for solid–liquid adsorption to describe the equilibrium data are the Langmuir, Freundlich, Dubinin–Radushkevich and Temkin isotherms.

The Langmuir model

According to Langmuir, the uptake occurs on a homogenous surface by monolayer adsorption with constant heat of adsorption for all sites and without interaction between adsorbed molecules. The Langmuir²² model is given as

$$q_e = \left[\frac{X_m b C_e}{1 + b C_e} \right] \quad (5)$$

where C_e is the equilibrium concentration of metal ion in the solution (mg L^{-1}), q_e is the amount of the metal ion adsorbed at equilibrium (mg g^{-1}), X_m is the amount of metal ion required to form a monolayer (i.e.,) adsorption capacity of the adsorbent (mg g^{-1}), and b (L mg^{-1}) is the equilibrium constant related to free energy or net enthalpy of adsorption ($b \propto e^{-\Delta H/RT}$). The above equation can be linearised and a plot of C_e/q_e versus C_e should be a straight line with slope $1/X_m$ and intercept $1/X_m b$ when adsorption follows the Langmuir model.

The Freundlich model

The Freundlich expression is an empirical equation based on adsorption on a heterogeneous surface. The Freundlich model does not indicate a finite sorbent uptake capacity and can only be applied in the low to intermediate concentration range. The general Freundlich²³ equation is as follows:

$$q_e = K_f (C_e)^{1/n} \quad (6)$$

where K_f (mg g^{-1}) and $1/n$ (L g^{-1}) are Freundlich isotherm constants relating multilayer adsorption capacity and adsorption intensity. The above equation is linearised and a plot of $\log q_e$ versus $\log C_e$ will give a straight line of slope $1/n$ and intercept K_f .

The Dubinin–Radushkevich model

The Dubinin–Radushkevich (D-R)²⁴ isotherm is more general because it does not assume a homogeneous surface or constant adsorption potential.

The D-R equation is given by,

$$q_e = q_m \exp(-K\varepsilon^2) \quad (7)$$

Its linear form can be represented as

$$\ln q_e = \ln q_m - K\varepsilon^2, \quad (8)$$

where q_e is the amount of the metal ion adsorbed at equilibrium, K is a constant related to the mean free energy of adsorption, q_m is the theoretical saturation capacity, ε is the Polanyi potential, equal to $RT \ln(1+(1/C_e))$. The values of q_m and K are determined by plotting $\ln q_e$ versus ε^2 .

The values of sorption energy (E_s) (kJ mol^{-1}) can be calculated from the equation,

$$E_s = \frac{1}{\sqrt{2K}} \quad (9)$$

If the magnitude of E_s is between 8 and 16 kJ mol^{-1} , the adsorption process proceeds by ion exchange or chemisorptions²⁵, while for values of $E_s < 8 \text{ kJ mol}^{-1}$, the adsorption process is of a physical nature²⁶.

The Temkin model

Temkin and Pyzhev²⁷ considered the effect of indirect interaction between the metal ions and adsorbent on adsorption isotherms. Because of these interactions, the heat of adsorption of all the molecules in the layer would decrease linearly with surface coverage. The Temkin equation is given as,

$$q_e = \frac{RT}{B} \ln(AC_e) \tag{10}$$

where, A ($L g^{-1}$) and B are Temkin constants relating to adsorption potential and heat of adsorption.

It can be linearized as follows,

$$q_e = \frac{RT}{B} \ln(A) + \frac{RT}{B} \ln(C_e) \tag{11}$$

A plot of q_e versus $\ln C_e$ gives the values of Temkin constants A and B .

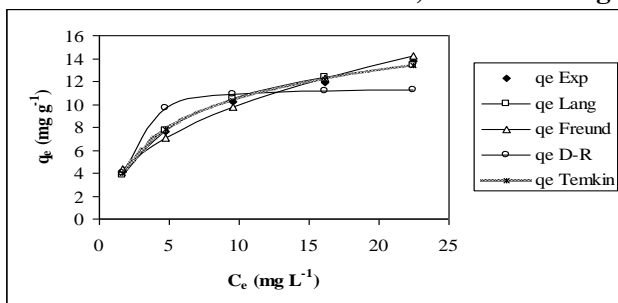
The isotherm constants and corresponding correlation coefficients are presented in (Table- 5).

Table 5: Isotherm constants for the adsorption of Zn on ACAS

Temp (K)	Langmuir constants			Freundlich constants			D-R constants				Temkin constants		
	X_m ($mg g^{-1}$)	b (Lmg^{-1})	R^2	n	K ($mg g^{-1}$)	R^2	K	q_m ($mg g^{-1}$)	R^2	E_s ($kJ mol^{-1}$)	B	A ($L g^{-1}$)	R^2
293	17.4216	0.2015	0.9834	2.2889	3.9555	0.989	0.5784	11.8509	0.8688	0.9298	0.6663	2.2225	0.9843
303	16.6945	0.1794	0.9927	2.2282	3.5304	0.9868	0.7226	11.393	0.8826	0.8318	0.7015	1.8533	0.9946
313	16.6667	0.1484	0.9875	2.1151	3.1003	0.9849	0.8941	11.0342	0.8825	0.7478	0.7127	1.4716	0.9882
323	16.6389	0.1177	0.9921	1.9794	2.6034	0.9839	1.2147	10.6398	0.9001	0.6416	0.7237	1.123	0.9935

It can be observed from (Table- 5), that the monolayer adsorption capacity decreased with an increase in temperature indicating the adsorption process to be exothermic. The experimental and theoretical values are compared and shown in (Figure- 9). As seen from the Figure, Langmuir, Freundlich and Temkin isotherm models fitted well with the experimental data. This was also shown by the higher regression coefficients obtained for Langmuir, Freundlich and Temkin isotherms.

Figure 9: Adsorption isotherms for Zn on ACAS, experimental and predicted by Langmuir, Freundlich, D-R and Temkin models at 303 K, ACAS loading $0.2g (100 mL)^{-1}$, pH 6, time 4h



The constant, b in (Table- 5) represents the affinity between the adsorbent and adsorbate. The values of b also showed a similar trend as X_m with temperature. The values of K_f from the Freundlich model are an indicator of the adsorption capacity of a given adsorbent. The adsorption intensity n in Freundlich model was greater than unity at various temperatures indicating favorable adsorption processes²⁸. The E_s value, suggests multilayer sorption behavior of Zn on ACAS. The Temkin isotherm also shows a higher correlation coefficient, which may be due to the linear dependence of heat of adsorption at low or medium coverages. This linearity may be due to the repulsion between adsorbate species or due to intrinsic surface heterogeneity.

Adsorption Kinetics

In the present study, the kinetics of the zinc ion removal was carried out to understand the behaviour of ACAS. The kinetics was analyzed by pseudo-first-order, pseudo-second-order and Elovich models at different temperatures.

Pseudo first order model

The pseudo first-order Lagergren model has been expressed as ²⁹,

$$\frac{dq_t}{dt} = K_1(q_e - q_t) \quad (12)$$

On integration, where $q_t = 0$ at $t = 0$, gives

$$\ln(q_e - q_t) = \ln(q_e) - K_1 t \quad (13)$$

where q_e and q_t refer to the amount of metal ion adsorbed per unit weight of adsorbent (mg g^{-1}) at equilibrium and at any time t (min). The value of q_e and first order adsorption rate constant K_1 (min^{-1}) can be obtained from the plot of $\ln(q_e - q_t)$ versus t .

Pseudo second order model

The pseudo second-order model is based on the assumption that adsorption follows a second-order mechanism. So, the rate of occupation of the adsorption sites is proportional to the square of the number of unoccupied sites. It can be given as³⁰,

$$\frac{dq_t}{dt} = K_2(q_e - q_t)^2 \quad (14)$$

Separating the variables and integrating; where $q_t = 0$ at $t = 0$ and $q_t = q_t$ at $t = t$, gives

$$\frac{t}{q_t} = \left[\frac{1}{K_2 q_e^2} + \frac{t}{q_e} \right] \quad (15)$$

The product $K_2 q_e^2$ is the initial sorption rate. A plot of t/q_t against t at different temperatures provides second order adsorption rate constants K_2 ($\text{g mg}^{-1} \text{min}^{-1}$) and q_e values from the slopes and intercept.

The Elovich model

One of the most useful models for the study of activated chemisorption is the Elovich equation. It is generally expressed as³¹,

$$\frac{dq_t}{dt} = \alpha \exp(-\beta q_t) \quad (16)$$

where q_t is the amount of solute adsorbed at time t , α is the initial adsorption rate ($\text{mg g}^{-1} \text{min}^{-1}$) β is the desorption constant (g mg^{-1}) during any one experiment. The Elovich equation can be simplified by assuming $\alpha \beta t \gg 1$ and applying the boundary conditions $q_t = 0$ at $t = 0$ and $q_t = q_t$ at $t = t$ Equation (16) becomes:

$$q_t = \left(\frac{1}{\beta} \right) \ln(\alpha \beta) + \left(\frac{1}{\beta} \right) \ln(t) \quad (17)$$

The Elovich constants α and β can be obtained from the plot of q_t vs $\ln(t)$.

The kinetic constants along with the correlation coefficients are listed in (Table- 6).

The experimental q_e values were compared to q_e values determined by the kinetic models. The Lagergren pseudo first-order rate constant K_1 and q_e determined from the model indicates that this model failed to estimate q_e since the experimental value of q_e differed from the estimated one. The regression coefficient values were found to be very less when compared to the other models. It was also observed that the theoretical adsorption capacity values ($1/\beta$) estimated from Elovich model did not agree well with the experimental q_e values and hence confirms that it is not appropriate to use this model to predict the adsorption kinetics for the removal of zinc ions using ACAS.

Table 6: Kinetic constants for the adsorption of Zn on ACAS

Temp (K)	Pseudo first order model			Pseudo second order model			Elovich model			q_e (exp) (mg g ⁻¹)
	q_e (cal) (mg g ⁻¹)	K_1 (min ⁻¹)	R^2	q_e (cal) (mg g ⁻¹)	K_2 (g mg ⁻¹ min ⁻¹)	R^2	β (g mg ⁻¹)	α (mg g ⁻¹ min ⁻¹)	R^2	
293	2.4018	0.024	0.8387	10.6045	0.06515	0.9998	3.0817	1.7E+11	0.969	10.5809
303	2.0907	0.019	0.7655	10.2041	0.07343	0.9998	2.9317	1.36E+10	0.9974	10.2050
313	2.2457	0.021	0.8243	9.9108	0.0718	0.9998	2.7020	6.72E+08	0.9969	9.8948
323	2.0629	0.0215	0.8153	9.251	0.0752	0.9998	3.2123	9.62E+09	0.9835	9.2369

The best fit for the experimental data of this study was achieved by the application of pseudo second-order kinetic equation³². It was observed that the model fitted the experimental data well. The coefficient of correlation for second-order kinetic model in Table 6 was greater than 0.99 and the estimated value of q_e also agreed with the experimental one. Both factors suggest that the adsorption of metal ions followed the second-order kinetic model, indicating that the rate-limiting step was a chemical adsorption process between zinc ion and ACAS. This provides the best correlation of the data. Therefore, this model can be applied for the entire adsorption process for the removal of metal ions.

Adsorption Mechanism

The prediction of the rate-limiting step is an important factor to be considered in the adsorption Process^{33, 34}. The three steps below analyze the mechanisms of adsorption as follows:

1. Transport of the solute from bulk solution through liquid film to the adsorbent exterior surface;
2. Transport of the adsorbate within the pores of the adsorbent (particle diffusion);
3. Adsorption of the adsorbate on the exterior surface of the adsorbent.

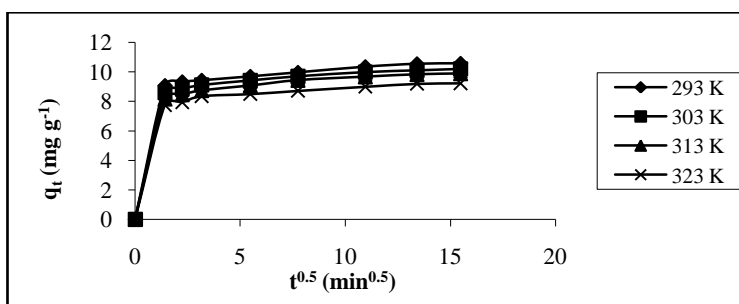
Generally, the last step is the equilibrium reaction and it is very rapid; the resistance is hence assumed to be negligible. The slowest step determines the rate-controlling parameter in the adsorption process. However, the rate-controlling parameter might be distributed between intraparticle and film diffusion mechanisms. Whatever may be the case, external diffusion will be involved in the adsorption process.

The most commonly used technique for identifying the mechanism involved in the adsorption process is by fitting the experimental data in an intraparticle diffusion plot. According to Weber and Morris³⁵, an intraparticle diffusion model can be given as

$$q_t = K_{id} t^{0.5} \quad (18)$$

where K_{id} is initial rate of the intra particle diffusion (mg (g min^{0.5})⁻¹). The value of K_{id} can be obtained from the slope of the plot of q_t versus $t^{0.5}$.

Figure 10: Intraparticle diffusion plot for the adsorption of Zn onto ACAS at different temperature, Initial Zn ion concentration 30 mg L⁻¹, ACAS loading 0.2 g (100 mL)⁻¹, pH 6



The plot of q_t versus $t^{0.5}$ for the adsorption of Zn on ACAS are shown in (Figure- 10), it represents the different stages of adsorption which characterizes the two or more steps involved in the sorption process. From the Figure, it can be noted that the adsorption process tends to follow two distinct trends. The two portions in

the intraparticle diffusion plot suggested that the adsorption process proceeded by film diffusion and intraparticle diffusion. The initial curved portion of the plot indicated a boundary layer effect i.e., film diffusion while the second linear portion was due to intraparticle or pore diffusion. The slope of the second linear portion of the plot has been defined as intraparticle diffusion rate constant, K_{id} . On the other hand, the intercept of the plot reflects the boundary layer effect. The larger the intercept, the greater was the contribution of the film diffusion to the rate limiting step. The calculated intraparticle diffusion rate constants K_{id} are listed in Table- 7. Average values of K_{id} were found to be in the order of 10^{-2} mg (g min^{0.5})⁻¹ for the adsorption of Zn on ACAS.

Table 7: Intraparticle diffusion rate parameter and diffusion coefficient for the adsorption of Zn on ACAS at different temperatures

S.No.	Temp (K)	$K_{id} \times 10^{+2}$ (mg g ⁻¹ min ^{-0.5})	$D_e \times 10^{+12}$ (m ² s ⁻¹)
1	293	11.86	3.1775
2	303	10.91	2.6041
3	313	10.54	2.4008
4	323	9.98	2.0639

Adsorption kinetic data obtained were further analyzed using the relationship between weight uptake and time in order to determine the rate-determining step of zinc ion adsorption onto ACAS. Assuming the adsorbent particle to be a sphere of radius 'r' and the diffusion follows Fick's law, the relationship between weight uptake and time is given by,

$$F(t) = 1 - \frac{6}{\pi^2} \sum_{n=1}^{\infty} \frac{1}{n^2} \exp[-n^2 Bt] \quad (19)$$

$$F(t) = \frac{q_t}{q_e} \quad (20)$$

where $F(t)$ is the fractional attainment of equilibrium at time t ,

$$B = \frac{\pi^2 D_e}{r^2} \quad (21)$$

where D_e is the effective diffusion coefficient (m² s⁻¹).

The K_{id} and diffusion coefficient values are presented in Table 7 and were found to decrease with increase in temperature. The values of D_e were found to be in the order of 10^{-12} m² s⁻¹. Srivastava et al.³⁶ reported D_e values of 6.848×10^{-13} m² s⁻¹ for the adsorption of Zn ions onto rice husk ash. The above values are comparable to the values obtained in the present study. For the present systems, the values of D_e fall well within the values reported in literature, specifically for the chemisorption systems (10^{-9} to 10^{-17} m² s⁻¹).

Conclusion:

The adsorption studies revealed that Agave sisalana fibre, an inexpensive material, could be used for the production of activated carbon using phosphoric acid as the activating agent for the removal of zinc ions from aqueous solutions. Zinc adsorption was found to be pH-dependent and maximum removal was observed at pH 6.0. The experimental and theoretical values were compared and from the results it was found that Langmuir, Freundlich and Temkin isotherm models fitted well with the experimental data. The kinetics of Zn ion adsorption were found to follow the pseudo-second-order model. The adsorption process was found to be controlled by both film diffusion and intra-particle diffusion. The data from the present study showed that the ACAS is indigenous, easily available material and has good potential in treating metal containing effluents.

References:

1. Manivasakam, N. "Industrial effluents Origin, characteristics, effects, analysis and treatment", Sakthi publication, 1987.
2. Athar, M. and Vohra, S. B. "Heavy metals and environment", Wiley Eastern Limited, New Delhi, 1995.
3. WHO, "Guidelines for Drinking Water Quality", World Health Organization, Geneva, Switzerland, Vol. 2, pp. 263, 1984.

4. Wang, J. and Chen, C. "Biosorbents for heavy metals removal and their future", *Biotechnology Advances*, Vol. 27, No. 2, pp. 195-226, 2009.
5. Kapoor, A. and Viraraghavan, T. "Fungal biosorption-An alternative treatment option for heavy metal bearing wastewaters: a Review", *Bioresource Technol.*, Vol. 53, No. 3, pp. 195-206, 1995.
6. Smith, E. H. "Uptake of heavy metals in batch system by a recycled iron bearing material", *Water Res.*, Vol. 30, No. 10, pp. 2424-2434, 1996.
7. Wigmans, T. "Industrial aspects of production and use of activated carbons", *Carbon*, Vol. 27, No. 1, pp. 13-22, 1989.
8. Helen Kalavathy, M., Karthikeyan, T., Rajgopal, S. and Lima Rose Miranda. "Kinetic and isotherm studies of Cu(II) adsorption onto H₃PO₄-activated rubber wood sawdust", *Journal of Colloid and Interface Science*, Vol. 292, No. 2, pp. 354-362, 2005.
9. Onyango, M. S., Kojima, Y., Aoyi, O., Bernardo, E. C. and Matsuda, H. "Adsorption equilibrium modeling and solution chemistry dependence of fluoride removal from water by trivalent-cation-exchanged zeolite F-9", *J. Colloid Interface Sci.*, Vol. 279, No. 2, pp. 341-350, 2004.
10. ASTM, "Standard test method for determination of iodine number of activated carbon", D 4607-94, pp. 1-5, 2006.
11. BIS, "Determination of decolorizing power", IS: 877-1977, pp. 9-10, 1977.
12. Chapman, H.D. "Cation exchange capacity", In: Black, C. A. (Ed.), *Methods of Soil Analysis*. Am. Inst. Agronomy, Madison, Wisconsin, Vol. 9, pp. 891-901, 1965.
13. Bansal, R. C., Donnet, J. B. and Stoeckli, F. "Active Carbon", Marcel Dekker, Inc., New York, 1988.
14. Washington, D. C. "Process design manual for carbon adsorption", Environmental Protection Agency (EPA), 1973.
15. Yu, L. J., Shukla, S. S., Dorris, K. L., Shukla, A. and Margrave, J. L. "Adsorption of chromium from aqueous solutions by maple sawdust", *J. Hazard. Mater.*, Vol. 100, No. 1-3, pp. 53-63, 2003.
16. Sthiannopkao, S. and Sreesai, S. "Utilization of pulp and paper industrial wastes to remove heavy metals from metal finishing wastewater", *Journal of Environmental Management*, Vol. 90, No. 11, pp. 3283-3289, 2009.
17. Martín-Lara, M. A., Hernainz, F., Calero, M., Blazquez, G. and Tenorio, G. "Surface chemistry evaluation of some solid wastes from olive-oil industry used for lead removal from aqueous solutions", *Biochemical Engineering Journal*, Vol. 44, No. 2/3, pp. 151-159, 2009.
18. Nasef, M. M. and Yahaya, A. H. "Adsorption of some heavy metal ions from aqueous solutions on Nafion 117 membrane", *Desalination*, Vol. 249, No. 2, pp. 677-681, 2009.
19. Mall, I. D., Srivastava, V. C., Agarwal, N. K. and Mishra, I. M. "Removal of congo red from aqueous solution by bagasse fly ash and activated carbon: Kinetic study and equilibrium isotherm analyses", *Chemosphere*, Vol. 61, No. 4, pp. 492-501, 2005.
20. Amarasinghe, B. M. W. P. K. and Williams, R.A. "Tea waste as a low cost adsorbent for the removal of Cu and Pb from wastewater", *Chem. Eng. J.*, Vol. 132, No. 1-3, pp. 299-309, 2007.
21. Farooq, U., Kozinski, J. A., Khan, M. A. and Athar, M. "Biosorption of heavy metal ions using wheat based biosorbents – A review of the recent literature", *Bioresource Technology*, Vol. 101, No. 14, pp. 5043-5053, 2010.
22. Langmuir, I. "The adsorption of gases on plane surfaces of glass, mica and platinum", *J. Am. Chem. Soc.*, Vol. 40, No. 8, pp. 1361-1403, 1918.
23. Freundlich, H. "Over the adsorption in solution", *Z. Phys. Chem.*, Vol. 57A, pp. 385-470, 1906.
24. Dubinin, M. M. "The potential theory of adsorption of gases and vapors for adsorbents with energetically non-uniform surface", *Chem. Rev.*, Vol. 60, pp. 235-266, 1960.
25. Ho, Y. S., Porter, J. F. and McKay, G. "Equilibrium Isotherm Studies for the sorption of divalent metal ions onto peat: Copper, nickel and lead single component systems", *Water Air Soil Pollut.*, Vol. 141, No. 1-4, pp. 1-33, 2002.
26. Onyango, M. S., Kojima, Y., Kumar, A., Kuchar, D., Kubota, M. and Matsuda, H. "Uptake of fluoride by Al³⁺ pretreated low-silica synthetic zeolites: Adsorption equilibrium and rate studies", *Sep. Sci. Technol.*, Vol. 41, No. 4, pp. 683-704, 2006.
27. Temkin, M. J. and Pyzhev, V. "Kinetics of ammonia synthesis on promoted iron catalysis", *Acta Physiochim.*, URSS, Vol. 12, pp. 327-356, 1940.
28. Agrawal, A., Sahu, K. K. and Pandey, B D. "Removal of zinc from aqueous solutions using sea nodule residue", *Colloids and Surfaces A: Physicochem. Eng. Aspects.*, Vol. 237, No. 1-3, pp. 133-140, 2004.
29. Lagergren, S. "Zur theorie der sogenannten adsorption gelöster stoffe, *Kungliga Svenska Vetenskapsakademiens*", *Handlingar*, Vol. 24, No. 4, pp. 1-39, 1898.
30. Ho, T. S. and McKay, G. "The Kinetics of sorption of basic dyes from aqueous solution by sphagnum moss peat", *Can. J. Chem. Eng.*, Vol. 76, No. 4, pp. 822-827, 1998.

31. Chien, S. H. and Clayton, W. R. "Application of Elovich equation to the kinetics of phosphate release and sorption on soils", Soil Sci. Soc. Am. J., Vol. 44, pp. 265-268, 1980.
32. Visa, M., Bogatu, C. And Duta, A. "Simultaneous adsorption of dyes and heavy metals from multicomponent solutions using fly ash", Applied Surface Science, Vol. 256, No. 17, pp. 5486-5491, 2010.
33. Sarkar, M., Acharya, P. K and Battacharya, B. "Modeling the adsorption kinetics of some priority organic pollutants in water from diffusion and activation energy parameters", J. Colloid Interface Sci., Vol. 266, No. 1, pp. 28-32, 2003.
34. Bhatnagar, A., Minocha, A. K. and Sillanpaa, M. "Adsorptive removal of cobalt from aqueous solution by utilizing lemon peel as biosorbent", Biochemical Engineering Journal, Vol. 48, No. 2, pp. 181-186, 2010.
35. Weber, W. J. and Morris, J. C. "Kinetics of adsorption on carbon from solution", J. San. Eng. Div., ASCE, Vol. 89, No. SA2, pp. 31-59, 1963.
36. Srivastava, V. C., Mall, I. D. and Mishra, I. M. "Characterization of mesoporous rice husk ash (RHA) and adsorption kinetics of metal ions from aqueous solution onto RHA", J. Hazard. Mater., Vol. B134, No. 1-3, pp. 257-267, 2006.
